AGU PUBLICATIONS

Journal of Advances in Modeling Earth Systems

RESEARCH ARTICLE

10.1002/2016MS000717

Key Points:
- A dynamic lake surface albedo scheme is added to the lake model
- The new lake model produces a more reasonable LST and LIC than the default lake model
- Ice melting and snow accumulation are important to simulating lake ice in the Great Lakes

Supporting Information:
- Supporting Information S1

Correspondence to:
C. Xiao,
cxiao@umich.edu

Citation:
Xiao, C., B. M. Lofgren, J. Wang, and P. Y. Chu (2016), Improving the lake scheme within a coupled WRF-lake model in the Laurentian Great Lakes, *J. Adv. Model. Earth Syst.*, *8*, doi:10.1002/2016MS000717.

Received 16 MAY 2016
Accepted 19 NOV 2016
Accepted article online 23 NOV 2016

© 2016. The Authors.
This is an open access article under the terms of the Creative Commons Attribution-NonCommercial-NoDerivs License, which permits use and distribution in any medium, provided the original work is properly cited, the use is non-commercial and no modifications or adaptations are made.

Improving the lake scheme within a coupled WRF-lake model in the Laurentian Great Lakes

Chuliang Xiao[1], **Brent M. Lofgren**[2], **Jia Wang**[2], **and Philip Y. Chu**[2]

[1]Cooperative Institute for Limnology and Ecosystems Research, University of Michigan, Ann Arbor, Michigan, USA, [2]NOAA Great Lakes Environmental Research Laboratory, Ann Arbor, Michigan, USA

Abstract In this study, a one-dimensional (1-D) thermal diffusion lake model within the Weather Research and Forecasting (WRF) model was investigated for the Laurentian Great Lakes. In the default 10-layer lake model, the albedos of water and ice are specified with constant values, 0.08 and 0.6, respectively, ignoring shortwave partitioning and zenith angle, ice melting, and snow effect. Some modifications, including a dynamic lake surface albedo, tuned vertical diffusivities, and a sophisticated treatment of snow cover over lake ice, have been added to the lake model. A set of comparison experiments have been carried out to evaluate the performances of different lake schemes in the coupled WRF-lake modeling system. Results show that the 1-D lake model is able to capture the seasonal variability of lake surface temperature (LST) and lake ice coverage (LIC). However, it produces an early warming and quick cooling of LST in deep lakes, and excessive and early persistent LIC in all lakes. Increasing vertical diffusivity can reduce the bias in the 1-D lake but only in a limited way. After incorporating a sophisticated treatment of lake surface albedo, the new lake model produces a more reasonable LST and LIC than the default lake model, indicating that the processes of ice melting and snow accumulation are important to simulate lake ice in the Great Lakes. Even though substantial efforts have been devoted to improving the 1-D lake model, it still remains considerably challenging to adequately capture the full dynamics and thermodynamics in deep lakes.

1. Introduction

Large water bodies such as the Laurentian Great Lakes can exert significant influences on local and regional climate, as open water typically has different radiative and thermal properties, compared to soil or vegetated surfaces, in terms of larger heat capacity, greater thermal conductance, lower albedo, and lower roughness [*Changnon and Jones*, 1972; *Bates et al*., 1993; *Scott and Huff*, 1996; *Lofgren*, 1997; *Notaro et al*., 2013].

The lakes' impact on the regional climate varies by season. In the ice-free season, the Great Lakes act as a vast moisture source with large thermal inertia, leading to a reduction of annual and diurnal air temperature ranges across the basin [*Bates et al*., 1993; *Scott and Huff*, 1996; *Notaro et al*., 2013]. The air-lake interaction can cause heavy precipitation on the downwind side, particularly during late autumn-early winter when cold air masses passing over the Great Lakes are warmed and moistened by the underlying water [*Bates et al*., 1993; *Wright et al*., 2013]. Furthermore, the lakes tend to intensify cyclones (anticyclones) during winter (summer) and weaken cyclones (anticyclones) during summer (winter) [*Cox*, 1917; *Notaro et al*., 2013; C. Xiao et al., WRF-based assessment of the Great Lakes' impact on cold season synoptic cyclones, submitted to *Journal of Geophysical Research: Atmospheres*, 2016]. In addition to the thermodynamic characteristics, the reduced roughness of the open water, compared to the surrounding land, enhances the surface wind, associated fetch, and the lake breeze. As temperate lakes, the Great Lakes exhibit a prominent seasonal cycle of lake surface temperature (LST) and lake ice coverage (LIC) [*Wang et al*., 2012], especially in winter time when the physical conditions of the lake surface change dramatically during the alternation between water and ice.

In regional climate models (RCMs), how to resolve LST and associated air-lake interactions is crucial to understanding the hydroclimate in water-dominated regions, i.e., the Great Lakes basin [*MacKay et al*., 2009; *Mallard et al*., 2015]. If no lake model is implemented in the lake grids, a "search" option in RCMs will be employed to extrapolate LST from the closest water point with valid data, e.g., Hudson Bay and the Atlantic Ocean, which can cause obvious biases and even adverse effects [e.g., *Spero et al*., 2016]. To bridge the gap,

Table 1. Summary of Select Prior Studies Using Lake Models in the Great Lakes

No.	Lake Model	Lakes	Ice	Coupling	References
1-D	Mixed-layer	All	Yes	Yes	*Goyette et al.* [2000]
	FLake	All	Yes		*Gula and Peltier* [2012] and *Mallard et al.* [2014]
	LETM	All		Yes	*Lofgren* [2004]
	Hostetler	All	Yes	Yes	*Hostetler et al.* [1993] and *Bates et al.* [1993]
	Hostetler	All	Yes	Yes	*Notaro et al.* [2013] and *Bennington et al.* [2014]
	Hostetler	Superior, Erie		Yes	*Gu et al.* [2015]
3-D	POM	Michigan			*Beletsky et al.* [2006]
	POM	Ontario			*Huang et al.* [2010]
	POM	Erie			*Beletsky et al.* [2013]
	POM	Erie	Yes		*Fujisaki et al.* [2013]
	FVCOM	Superior			*Xue et al.* [2015]
	NEMO	All	Yes		*Dupont et al.* [2012]
	FVCOM	All			*Bai et al.* [2013]

a variety of lake models with different complexities has been performed in the Great Lakes (Table 1): a slab-type thermodynamic model, the Mixed-Layer Model [*Goyette et al.*, 2000]; and the Large Lake Thermodynamics Model (LLTM) [*Croley*, 1989; *Lofgren*, 2004]; a relatively simple two-layer model based on similarity theory, FLake [*Gula and Peltier*, 2012; *Mallard et al.*, 2014]; a thermal diffusion model with parameterized eddy diffusivity, the one-dimensional (1-D) Hostetler model [*Hostetler et al.*, 1993; *Bates et al.*, 1993; *Stepanenko et al.*, 2010; *Notaro et al.*, 2013; *Bennington et al.*, 2014]. Meanwhile, ocean general circulation models (OGCMs) have been adapted to the Great Lakes. The Princeton Ocean Model (POM) serves as one of the most popular implementations to develop lake models for the Great Lakes, but focusing on individual lakes [*Beletsky et al.*, 2006; *Huang et al.*, 2010; *Beletsky et al.*, 2013; *Fujisaki et al.*, 2013]. Recently, an unstructured Finite-Volume Community Ocean Model (FVCOM) has attracted increasing attention [e.g., *Xue et al.*, 2015]. Given that a basin-scale hydrodynamic model is needed to understand the climate response in the Great Lakes region, others have tried to integrate all lakes in one OGCM, such as Nucleus for European Modeling of the Ocean (NEMO) [*Dupont et al.*, 2012], and FVCOM [*Bai et al.*, 2013]. In contrast to those 1-D lake models that are generally coupled with atmospheric models, 3-D lake models are currently running stand-alone for the Great Lakes.

The Weather Research and Forecasting (WRF) model with the Advanced Research WRF (ARW) dynamic core [*Skamarock et al.*, 2008] is widely used in regional modeling communities. As a limited area, nonhydrostatic model, with a terrain-following Eta-coordinate mesoscale modeling system, WRF has been designed to serve both operational forecasting and atmospheric research needs. Prior to 2013, WRF required prescribed surface temperatures in the water grids from the driven data; otherwise, the "search" option would have been activated. Starting with version 3.6, WRF has been incorporated with a thermal diffusion lake model. The vertical diffusivity of this lake model was calibrated by *Gu et al.* [2015], based on single buoy observations for two individual lakes (Superior and Erie) and only focused on the ice-free period. In the default lake model, the albedos of water and ice were specified with constant values, 0.08 and 0.6, respectively, ignoring solar zenith angle and shortwave radiation diffusion, ice melting, and snow effect. In this study, a set of comparison experiments were carried out to evaluate the coupled WRF-lake model's performance for the entire Great Lakes system. In one experiment, the lake model was modified by introducing a new dynamical lake surface albedo.

The remainder of this paper is organized as follows. The model modification is described in section 2. The data sets, model configurations, and experimental designs are introduced in section 3. Modeling results are analyzed in section 4. Discussion and conclusions are presented in section 5.

2. Method

2.1. Overview of the 1-D Lake Model in WRF

The thermal diffusion lake model, denoted as the *Lake, Ice, Snow and Sediment Simulator* (LISSS) [*Subin et al.*, 2012], was inserted into the Community Land Model (CLM) 4.5 [*Oleson et al.*, 2013] with calibrations from *Gu et al.* [2015], based on the original concept of *Hostetler and Bartlein* [1990]. It is a 1-D mass and energy balance scheme with 20–25 model layers, including up to 5 snow layers on the lake ice, 10 water layers, and

10 soil layers on the lake bottom. The lake scheme is implemented with actual lake bathymetries derived from the global gridded lake data set provided by *Kourzeneva et al*. [2012]. The lake scheme is independent of a land surface scheme and therefore can be used with any land surface scheme embedded in WRF. Although the study is restricted to the Great Lakes and the WRF model, the physical insights gained can be extended to other types of lakes and RCMs.

The governing equation for the 1-D lake model is based on *Hostetler and Bartlein* [1990]

$$\frac{\partial T}{\partial t}=\frac{\partial}{\partial z}\left\{[\kappa_m+K_{ed}]\frac{\partial T}{\partial z}\right\}+\frac{1}{C_w}\frac{\partial \Phi}{\partial z}, \tag{1}$$

where T, t, z, κ_m, K_{ed}, C_w, and Φ are water temperature (K), time (s), depth from the surface (m), the molecular diffusion of water ($m^2\ s^{-1}$), eddy diffusion ($m^2\ s^{-1}$), the volumetric heat capacity of water ($J\ m^{-3}\ K^{-1}$), and a heat source term ($W\ m^{-2}$), respectively.

2.2. Eddy Diffusion

For unfrozen lakes, the eddy diffusivity K_{ed} is evaluated at each depth as a function of the 2 m wind speed, the Brunt-Väisälä frequency, and the latitude-dependent Ekman decay, using the method of *Henderson-Sellers* [1985].

To compensate for missing 3-D mixing processes, additional background mixing, namely enhanced diffusion, is incorporated to the 1-D vertical diffusion [*Fang and Stefan*, 1996; *Subin et al*., 2012; *Bennington et al*., 2014].

As documented in *Martynov et al*. [2010], the 1-D lake model could produce realistic temperature profiles in shallow lakes, but performed poorly in lakes with depths greater than 50 m, where a much stronger mixing might be required to provide a reasonable simulation. *Subin et al*. [2012] suggested that the eddy diffusivity K_{ed} should be enhanced by factors of 10–100 in deep lakes. To account for the vertical convection, *Gu et al*. [2015] increased K_{ed} by a larger factor when LST was equal to or less than 4°C but greater than the freezing point in deep lakes, which now is the default calculation of vertical diffusivities in the 1-D lake model of WRF.

2.3. Modifications

Several surface processes have been added to the 1-D lake model, including the calculation of the diffuse solar radiation and the lake surface albedo.

2.3.1. Diffuse Solar Radiation

To differentiate the direct and diffuse solar radiation, a simple shortwave partitioning parameterization [*San Jose et al*., 2011] is introduced in the lake model. The parameterization was included in the Eulerian/semi-Lagrangian fluid solver (EULAG)-computational fluid dynamics (CFD) model, which was further adapted in the coupled WRF-EULAG/CFD-urban model [*Chen et al*., 2011]. The diffuse radiation is calculated as the total radiation multiplied by a turbidity factor (TF) defined as the relation between extraterrestrial solar radiation (S_{Top}) and the incoming solar radiation over the horizontal plane (S_{Down}). The TF is calculated as follows:

$$S_{Top}=S_{Con}\times\cos z, \tag{2}$$

$$B=2.1-2.8\times\ln\left(\ln S_{Top}/S_{Down}\right), \tag{3}$$

$$A=max(0.1,\ \ B), \tag{4}$$

$$TF=min(1,\ \ 1/A), \tag{5}$$

where S_{Con} is the solar constant and z is the zenith angle.

2.3.2. Lake Surface Albedo

In the default lake model, the albedos of water and ice are specified with constant values, 0.08 and 0.6, respectively,

$$a=0.6\times f_{ice}+(1-f_{ice})\times 0.08, \tag{6}$$

where a is the albedo and f_{ice} the LIC fraction. In the following subsection, a dynamical lake surface albedo with a special treatment of snow cover over lake ice was incorporated in the lake model.

2.3.2.1. Water Lake Surface

When the lake surface temperature (T_g) is above freezing (T_f), the albedo (a_w) for the direct shortwave radiation is calculated in the form of *Pivovarov* [1972] while the albedo (a_w^{μ}) for the diffuse radiation is set to 0.1, which can be calculated as an integral over all angles of the full sky,

$$a_w = \frac{0.05}{\cos z + 0.15}, \quad a_w^{\mu} = 0.1. \tag{7}$$

2.3.2.2. Frozen Lake Without Snow

For the frozen lake ($T_g < T_f$) with snow depth <40 mm, the albedo is set to 0.6 for visible radiation ($a_{0,vis}$) and 0.4 for near-infrared radiation ($a_{0,ir}$), same as in *Subin et al.* [2012],

$$a_{0,vis} = 0.6, \quad a_{0,ir} = 0.4. \tag{8}$$

To account for the liquid water above the ice, the albedo of ice (a_{ice}) is reduced as suggested by *Mironov et al.* [2010],

$$a_{ice} = a_0(1-x) + 0.10x, \quad x = \exp\left(-95\left(T_g - T_f\right)/T_f\right), \tag{9}$$

$$a_{ice} = max\left(a_{ice}, a_w\right). \tag{10}$$

2.3.2.3. Frozen Lake With Snow

When snow is present on the ice with snow depth >40 mm, the albedo is calculated as the area-weighted average between ice and snow. Following *Andreadis et al.* [2009], the snow albedo is assumed to decay with age

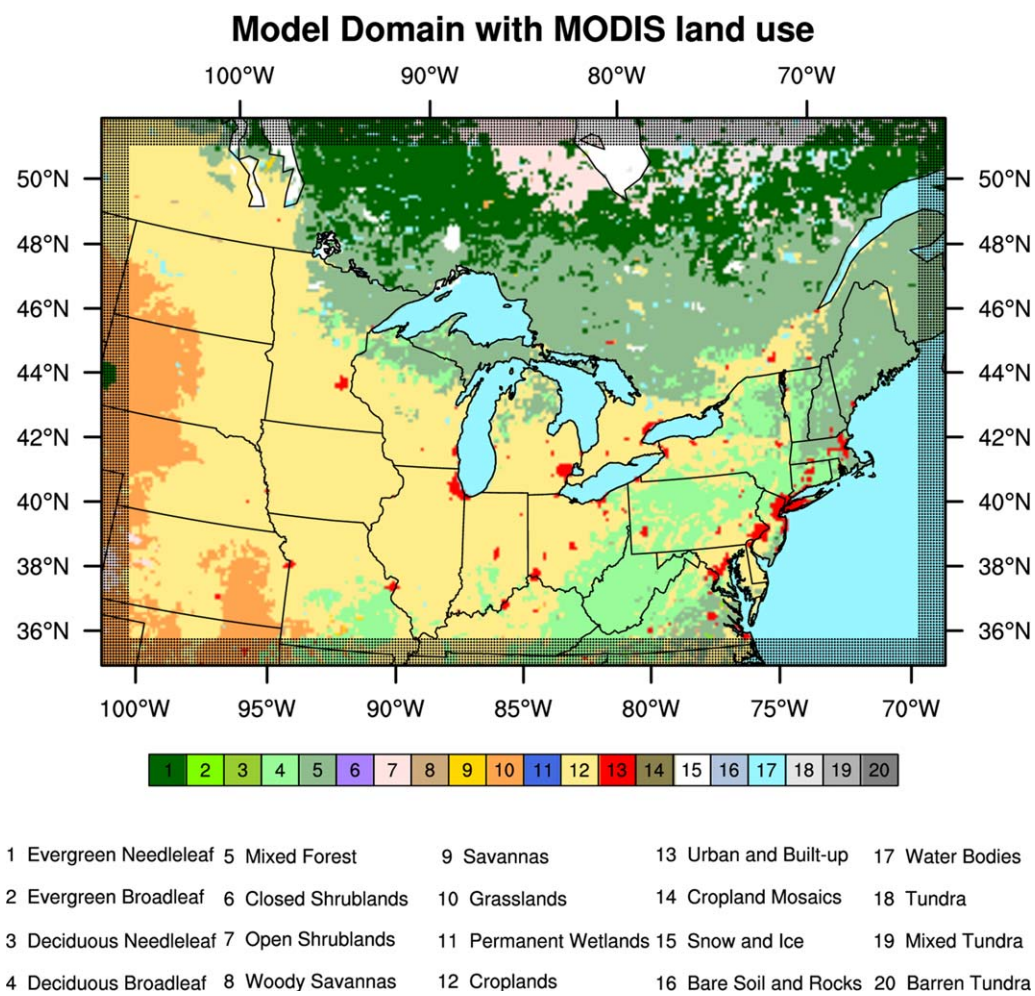

Figure 1. The WRF model domain with MODIS land use categories. The lateral buffer zone is marked with dots.

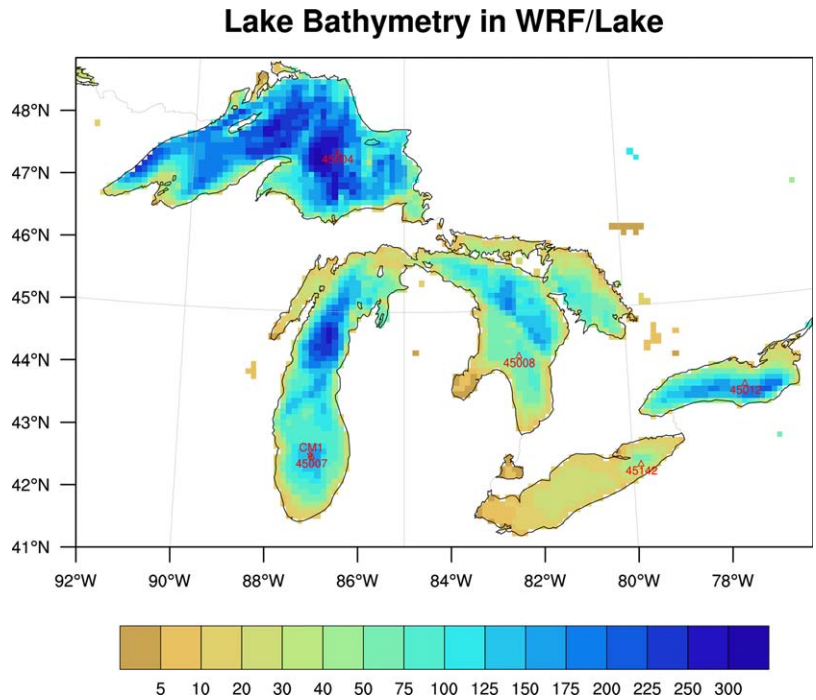

Figure 2. The bathymetry (m) of the Great Lakes in the 1-D Lake model on a 10 km spatial spacing grid. The NOAA National Data Buoy Center (NDBC) buoy stations are marked with triangles. The Mooring station in Lake Michigan is labeled as CM1.

$$a_{snw,accu}=0.85\lambda_a^{t^{0.58}},\quad \lambda_a=0.92, \tag{11}$$

$$a_{snw,melt}=0.85\lambda_a^{t^{0.46}},\quad \lambda_a=0.70, \tag{12}$$

where t is the time since the last snowfall (in days).

3. Data Sets and Experimental Design

3.1. Data Sets

3.1.1. Reanalysis Data

The initial and lateral boundary conditions for the WRF-lake model were provided by the 3 h National Centers for Environmental Prediction North American Regional Reanalysis (NARR) on a 32 km spatial grid (http://rda.ucar.edu/datasets/ds608.0/) [*Mesinger et al.*, 2006].

3.1.2. Lake Surface Temperature and Ice Coverage

The simulated LST from the 1-D lake model was assessed against the National Oceanic and Atmospheric Administration (NOAA) Great Lakes Surface Environmental Analysis (GLSEA) data set from the Advanced Very High Resolution Radiometer [*Schwab et al.*, 1992]. NOAA's Great Lakes Ice Atlas [*Wang et al.*, 2012] was applied to evaluate the simulation of LIC.

3.1.3. Vertical Temperature Profile in Lake Michigan

Moored thermistor strings continually measure water temperatures at varying depths, which provides site-specific subsurface data to validate the model's vertical thermal structure. The vertical water temperature observations from southern Lake Michigan's central basin (42°40.493′N, 87°04.772′W) (CM1 Station in Figure 2) have been measured since 1990 [*McCormick and Pazdalski*, 1993]. The location was based on its proximity to NOAA National Data Buoy Center (NDBC)

Table 2. Parameterization Schemes Used in the Setup of WRF

Physics	Scheme	References
Microphysics	WRF Single-Moment 6-class	*Hong and Lim* [2006]
Cumulus convection	Kain-Fritsch	*Kain* [2004]
Shortwave, longwave	CAM	*Collins et al.* [2004]
Planetary boundary layer	Yonsei University	*Hong et al.* [2006]
Land surface model	Community Land Model	*Oleson et al.* [2013]

Table 3. The Configuration of Numerical Experiments

Experiments	Diffusivity	Albedo	Layers
Lake_CTL	Default, as calibrated by *Gu et al.* [2015]	Default	10
Lake_OLD	Original, as in *Hostetler and Bartlein* [1990]	Default	10
Lake_CLM	Suggested by *Subin et al.* [2012] in CLM4.5	Default	10
Lake_NEW	Default, as in *Gu et al.* [2015]	New	10
Lake_EXT	Default, as in *Gu et al.* [2015]	New	25

buoy 45007 and reasonable range to vessel maintenance support. In this study, the observational data for 2011 (the last available year) was used to validate the lake model's thermal structure. In this year, the thermistors were located at the following depths (m): 6.9, 11.9, 16.9, 21.9, 26.9, 36.9, 57.9, 77.9, 97.9, 117.9, and 147.5. The monthly temperature was averaged from the original hourly observation.

3.1.4. Additional Data Sets

To validate the WRF model's performance, in addition to the NARR reanalysis, three observational precipitation data sets were also used: the Oak Ridge National Laboratory DayMet at 1 km horizontal grid resolution [*Thornton et al.*, 2016], the 2.5° × 2.5° global monthly CPC Merged Analysis of Precipitation (CMAP) [*Xie and Arkin*, 1997], and the Global Precipitation Climatology Project (GPCP) version 2.2 on a 2.5° global grid [*Adler et al.*, 2003].

3.2. WRF Configurations

The WRF-ARW model version 3.6.1 (hereafter referred to as WRF), interactively coupled with the 1-D lake model, was employed in this study. The WRF-lake model was run on a single domain with a grid spacing of 10 km (Figure 1) and 31 vertical levels. The sea surface temperature in Hudson Bay and the Atlantic Ocean

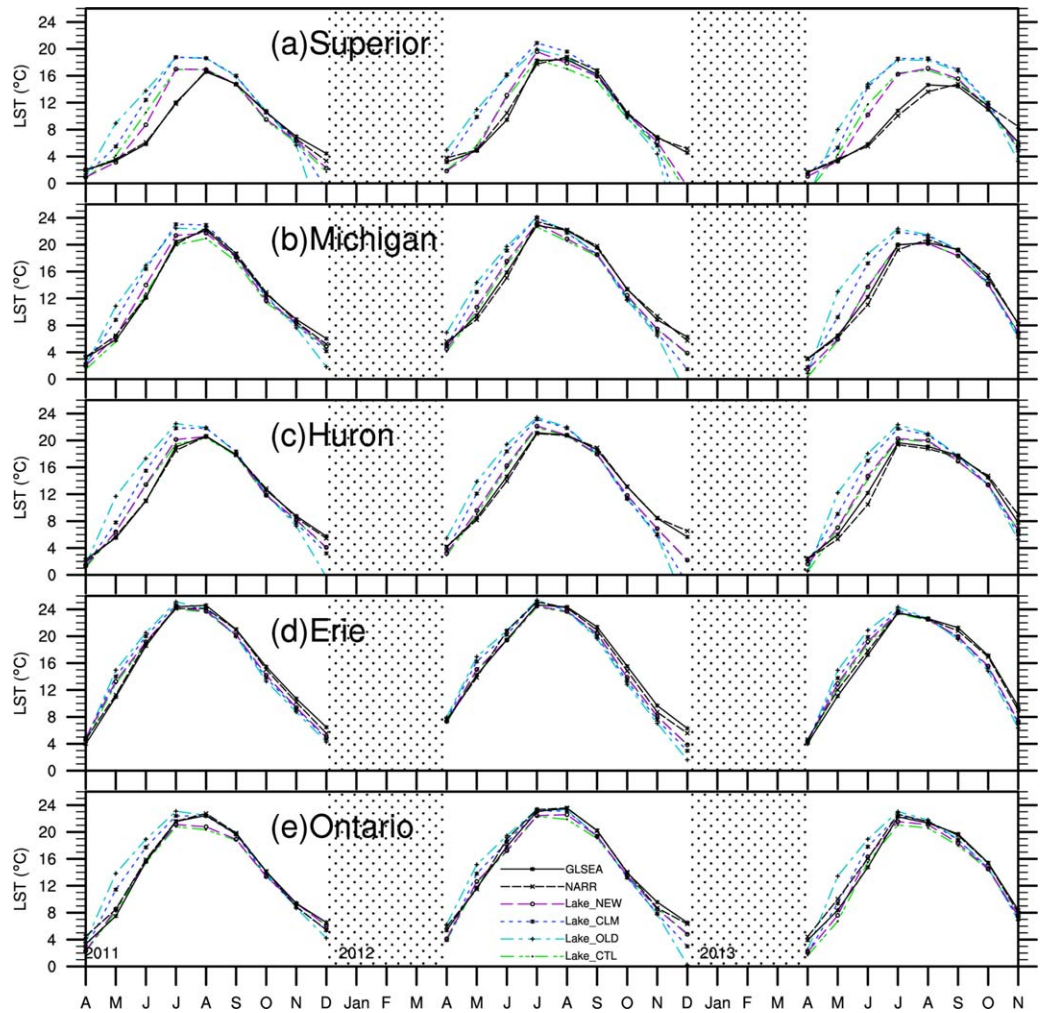

Figure 3. Monthly lake-mean LST (°C) from April 2011 to November 2013 simulated by different lake schemes. The lake surface temperature in the months (December–April) with ice is omitted.

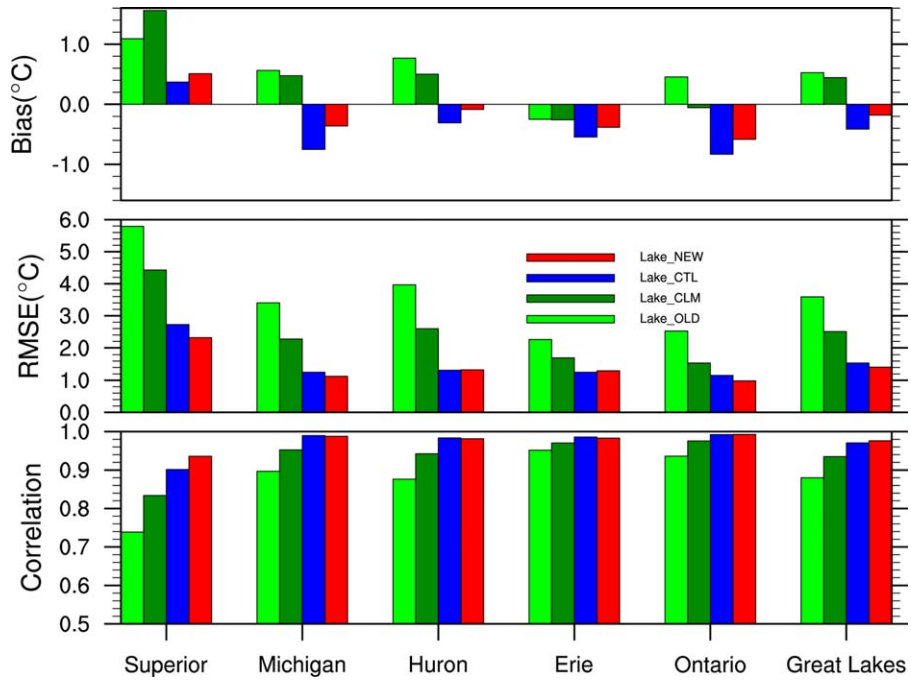

Figure 4. Statistical features of the discrepancy between simulated and observed LSTs during ice-free time (Figure 3). Bias denotes the 26 month mean of each simulation minus GLSEA. Root Mean Square Error (RMSE) and correlation coefficient are calculated between each simulation and GLSEA.

was provided by the NARR skin temperature and was updated every 3 h, while the LST in the Great Lakes was calculated internally by the 1-D lake model. At the current grid spacing, the Great Lakes are well represented in the lake model (Figure 2). The complete suite of physics parameterization schemes is listed in Table 2. The domain's lateral boundary was formulated with a one-point specified zone and a nine-point relaxation zone (Figure 1). A weak spectral nudging (maximum wave number 3) was applied at all levels above the planetary boundary layer, preventing synoptic-scale climate drift and also maintaining the objective of downscaling to be consistent with NARR.

3.3. Experimental Design

A series of numerical experiments was designed to evaluate the performance of different lake schemes in the coupled WRF-lake modeling system (Table 3): the control run, Lake_CTL, using the default scheme; two sensitivity runs, Lake_OLD and Lake_CLM, using the original and enhanced eddy diffusivities K_{ed}, respectively; the new run, Lake_NEW, using the new albedo scheme introduced in section 2.3; finally, the extralayer run, Lake_EXT, using 25 vertical layers (see details in section 4.5). The experiments were run from 1 January 2010 to 1 July 2014. We analyzed the period from 2011 to 2014, covering three winters with different climate regimes: the extremely warm winter 2011/2012, the slightly cooler than normal winter 2012/2013, and the extremely cold winter 2013/2014.

4. Results

4.1. Lake Surface Temperature

Simulated monthly lake-mean LST during ice-free time was compared with the GLSEA observation and the lake skin temperature in NARR (Figure 3). Generally, all lake model configurations produced plausible seasonal evolutions, as well as the interlake comparisons, of LST, performing better in the shallow lakes (Erie and Ontario) than in the deep lakes (Superior, Michigan, and Huron). The biggest discrepancy occurs in spring and early summer time when the 1-D lake model produced an earlier stratification, especially in Lake Superior. As documented in *Gu et al.* [2015], increasing vertical diffusivity can delay the stratification in the 1-D lake model. The comparison between Lake_CTL and Lake_NEW shows that incorporating a new surface albedo makes the lake model more realistic. The statistic comparisons between simulated and overserved

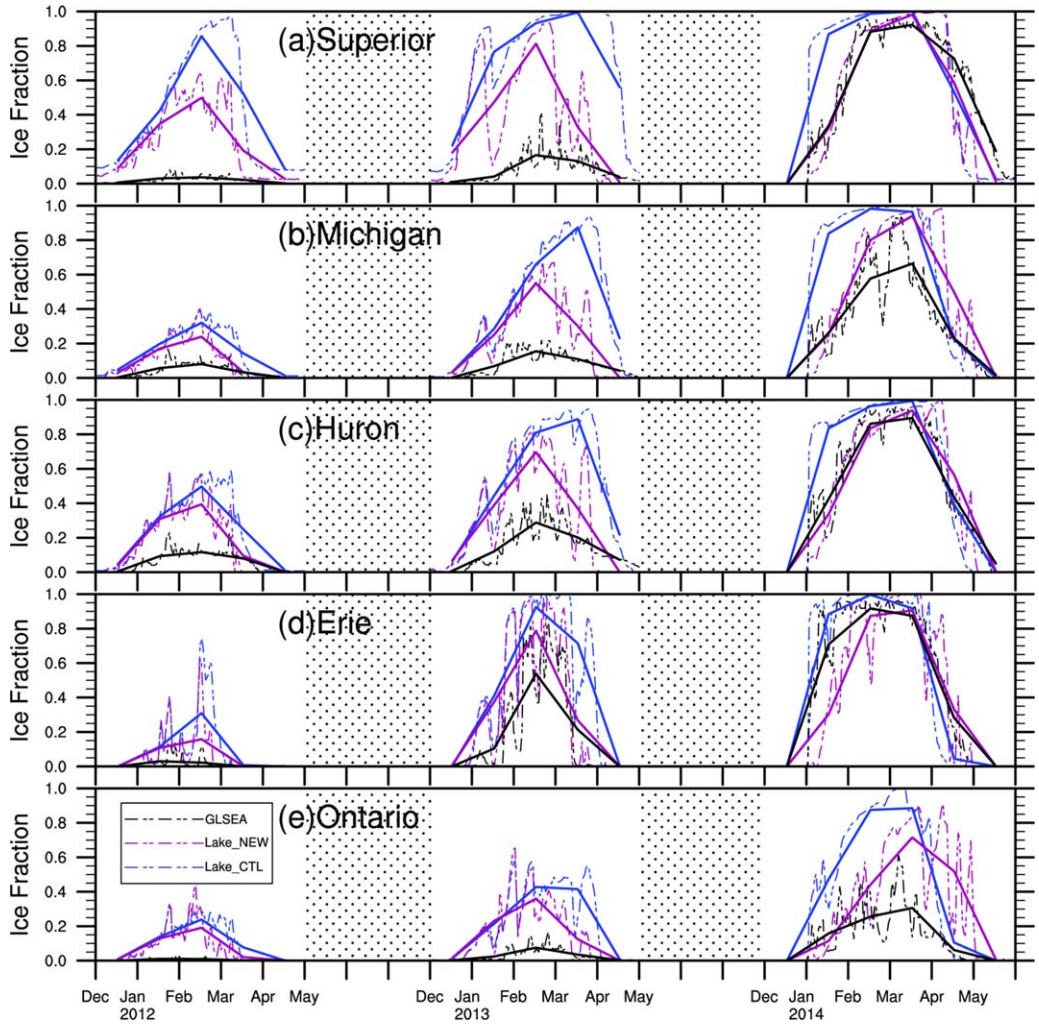

Figure 5. Monthly lake-mean LIC in three winters simulated by the default lake model (Lake_CTL, blue) and the new lake model (Lake_NEW, purple), compared with the GLSEA observation (black). The solid curves are the monthly average of their corresponding dashed curves.

LSTs in each lake are listed in Figure 4. The original *Hostetler and Bartlein* [1990] lake model (Lake_OLD) overestimated the LST in every lake except for Lake Erie, which was much improved by the LISSS (Lake_CLM). The lake model's bias was further reduced after *Gu et al*. [2015]'s calibration (Lake_CTL). With the surface albedo, the Lake_NEW model improved the simulation of both the mean state (expect for Lake Superior) and the variability of the LST in all lakes, and had a better correlation with the observation than the Lake_CTL model. The lake model, constrained by its single spatial dimension, still cannot adequately produce the LST in deep lakes. The discrepancy of LST can be partially attributed to the air temperature bias in the atmospheric component of the system.

4.2. Lake Ice Coverage

In the previous work of *Gu et al*. [2015], the lake ice was not considered. Here the LIC simulated by Lake_CTL and Lake_NEW is assessed against the Great Lakes Ice Atlas. Note that the concept of the LIC in the 1-D lake model expressed as the lake ice fraction is different with that in the satellite-retrieved observation. The lake model assumes that all ice is at the top of the lake [*Subin et al*., 2012]. For model layers containing both water and ice, the ice is assumed to be stacked vertically on top of the water. In the 10-layer lake model, the top model layer is set at a fixed depth of 0.05 m and the thickness of the first layer is 0.1 m. The ice fraction is calculated as the volume of ice frozen divided by the total volume of the top layer in the grid cell.

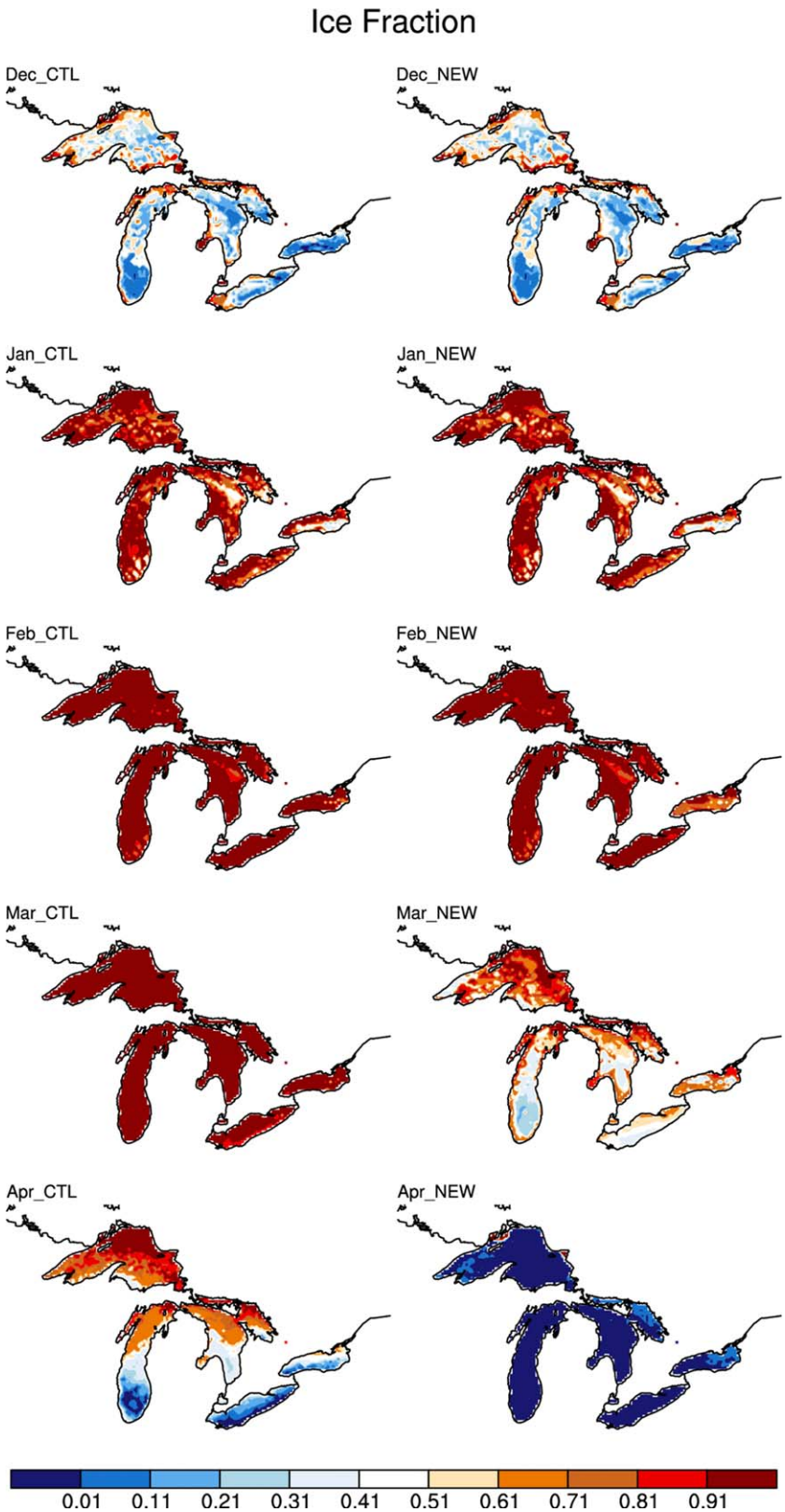

Figure 6. Lake ice fraction from December 2012 to April 2013 simulated by the default lake model (Lake_CTL) and the new lake model (Lake_NEW).

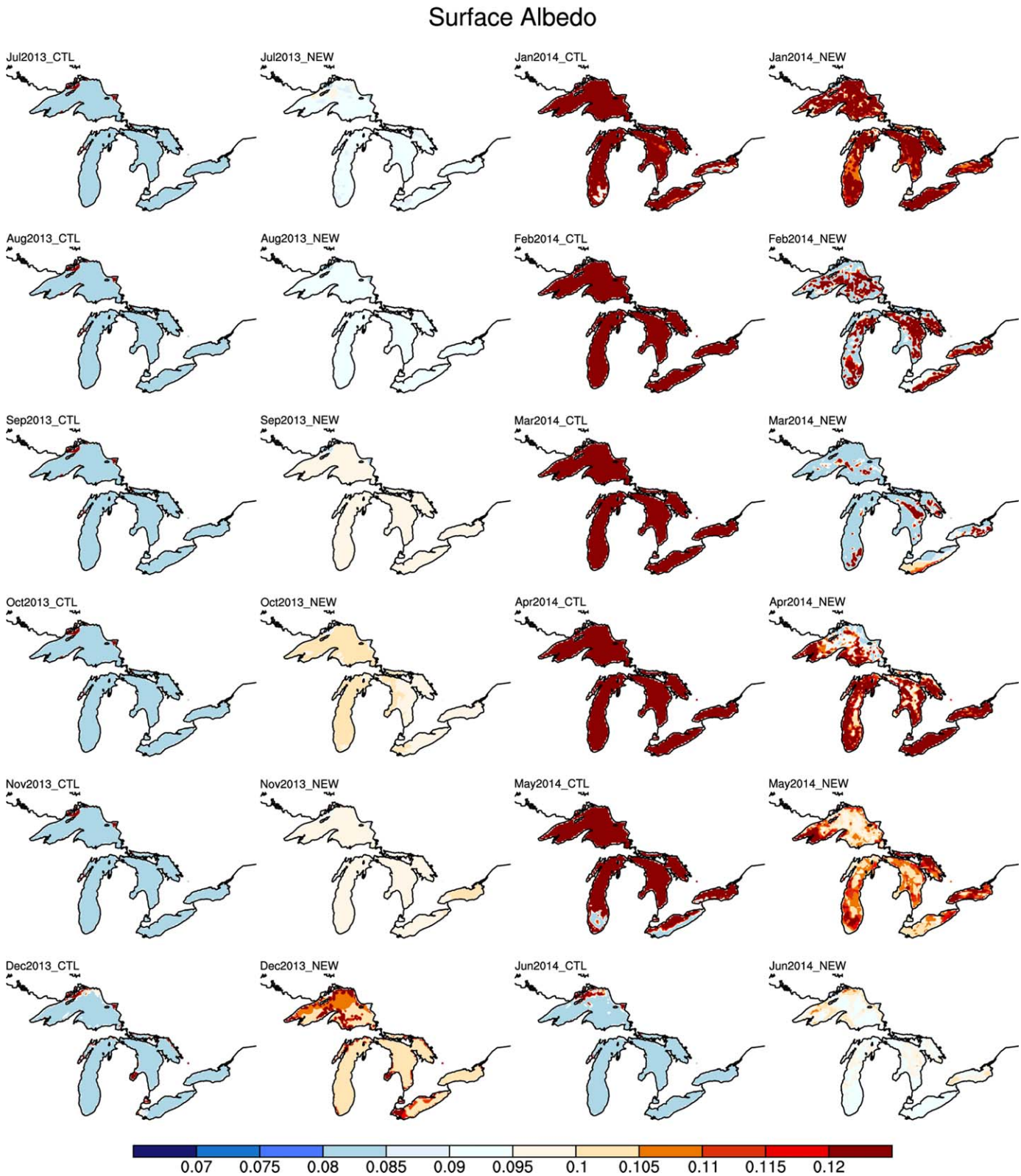

Figure 7. Monthly lake surface albedos from July 2013 to June 2014 by the default lake model (Lake_CTL) and the new lake model (Lake_NEW).

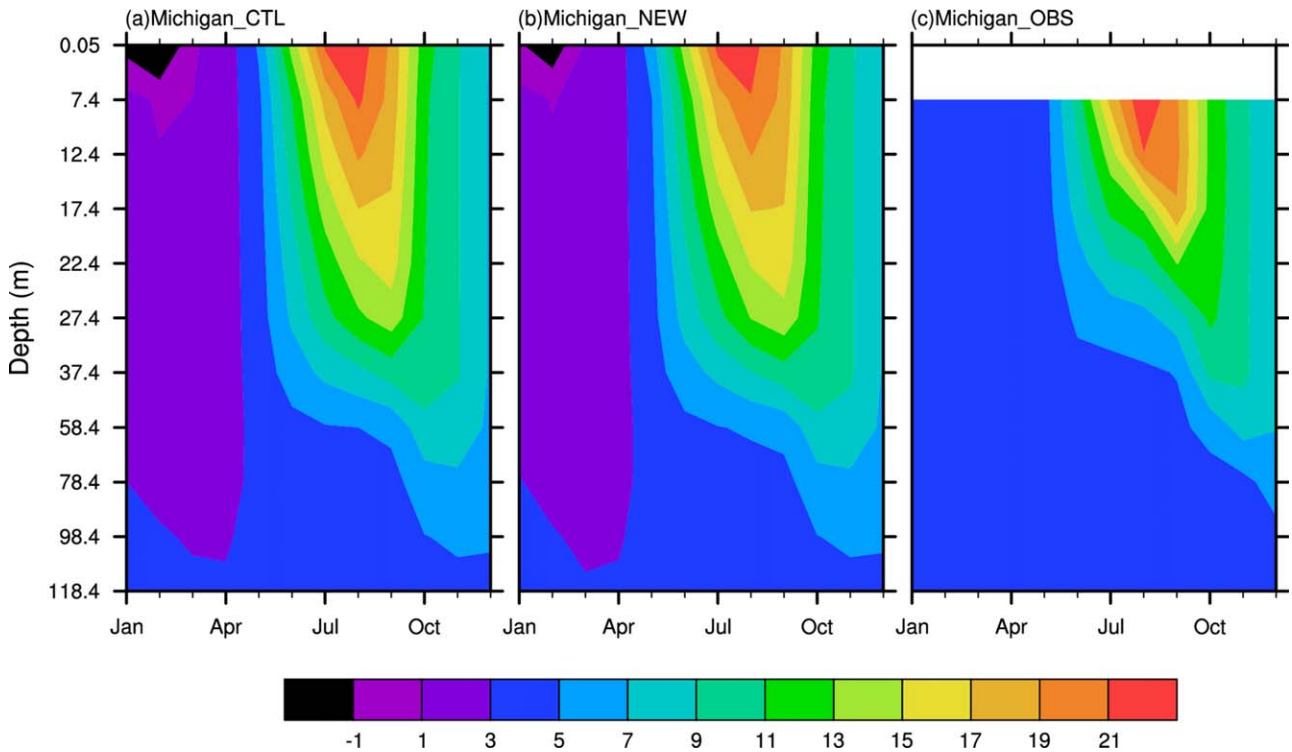

Figure 8. Vertical profiles of water temperature (°C) at a middle Lake Michigan station simulated by Lake_CTL and Lake_NEW in 2011, compared to the mooring observation (OBS).

For example, the value 70% of ice fraction means that if it were spread evenly over the entire grid cell, the top 0.07 m of the first layer would be frozen.

Figure 5 shows the simulated and observed lake-mean LIC for each lake. The LIC in the Great Lakes exhibits a remarkable interannual variability. The annual maximum LIC is 12.9% in 2011/2012, 38.4% in 2012/2013, and 92.5% in 2013/2014. The default lake model produced excessive ice in the top layer. After the dynamic albedo scheme was incorporated in the lake model, not only the maximum of LIC was reduced but also the intraseasonal fluctuation of LIC was reasonably reproduced. The new lake model had a better performance in capturing the ice decaying process, attributed to the treatment of the snow age and ice melting. The spatial distribution of LIC simulated by the lake models are compared in Figure 6. In the ice buildup time from December to February, similar lake ice coverages were produced by the default and the new lake models. Notable differences first occurred in March, especially in the lower lakes, when inordinate ice was maintained in Lake_CTL but was obviously reduced in Lake_NEW. In April, Lake Superior and northern parts of Michigan-Huron were still frozen in Lake_CTL, while all lakes were almost ice-free in Lake_NEW. Although significant improvements have been achieved in the new lake model, it still remains considerably challenging for the 1-D lake model to simulate the LIC in the Great Lakes.

4.3. Lake Surface Albedo

Since most of our modifications aimed at surface processes, we further examined the lake surface albedo (Figure 7). During the ice-free months, there were almost identical albedos in the Lake_CTL experiment, in which the albedo of water surface was set to a constant value 0.08. The Lake_CTL experiment, with the updates of the water surface albedo changing with the zenith angle and taking into account the diffuse radiation, produced a varying surface albedo, higher than that in the Lake_CTL experiment. As shown in Figure (3 and 1)-D lake models overestimated the LST during spring and early summer. The new lake model with a higher albedo tends to mitigate the overwhelming warming of LST by reducing the input radiation. When the lake became iced, the albedo changed from 0.08 to 0.6 in Lake_CTL, making a striking jump from December to January. As long as the ice was present, the albedo would be maintained via a positive ice-albedo feedback, where increasing ice cover can increase the albedo, reducing the amount of solar energy absorbed and leading to more ice. In addition to increasing the water albedo to delay the stratification in the ice-free time, the new scheme in Lake_NEW significantly decreased the lake surface albedo when ice

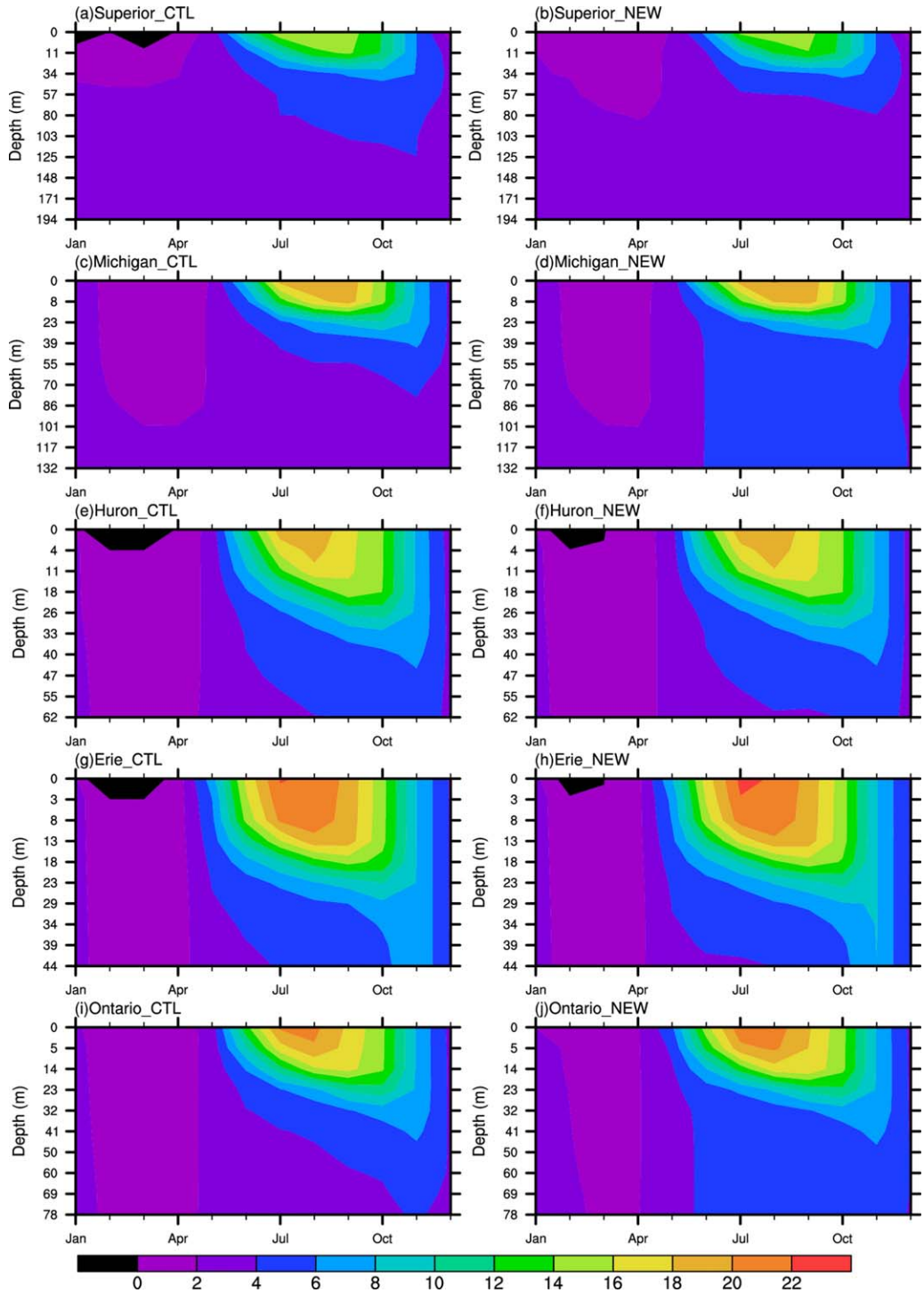

Figure 9. Vertical profiles of water temperature (°C) at different stations in each lake simulated by Lake_CTL and Lake_NEW in 2012.

was present in the lakes. Because of the lower albedo, more radiation was absorbed in the lake surface and the lake ice was therefore reduced. By introducing the new surface albedo scheme, more reasonable LST and LIC were produced in the Lake_NEW experiment relative to the Lake_CTL experiment.

4.4. Vertical Temperature Profile

Besides the surface properties, the vertical profile of water temperature in the 1-D lake model is assessed against a mooring observation located in the middle of Lake Michigan (Figure 8). The model layer depths

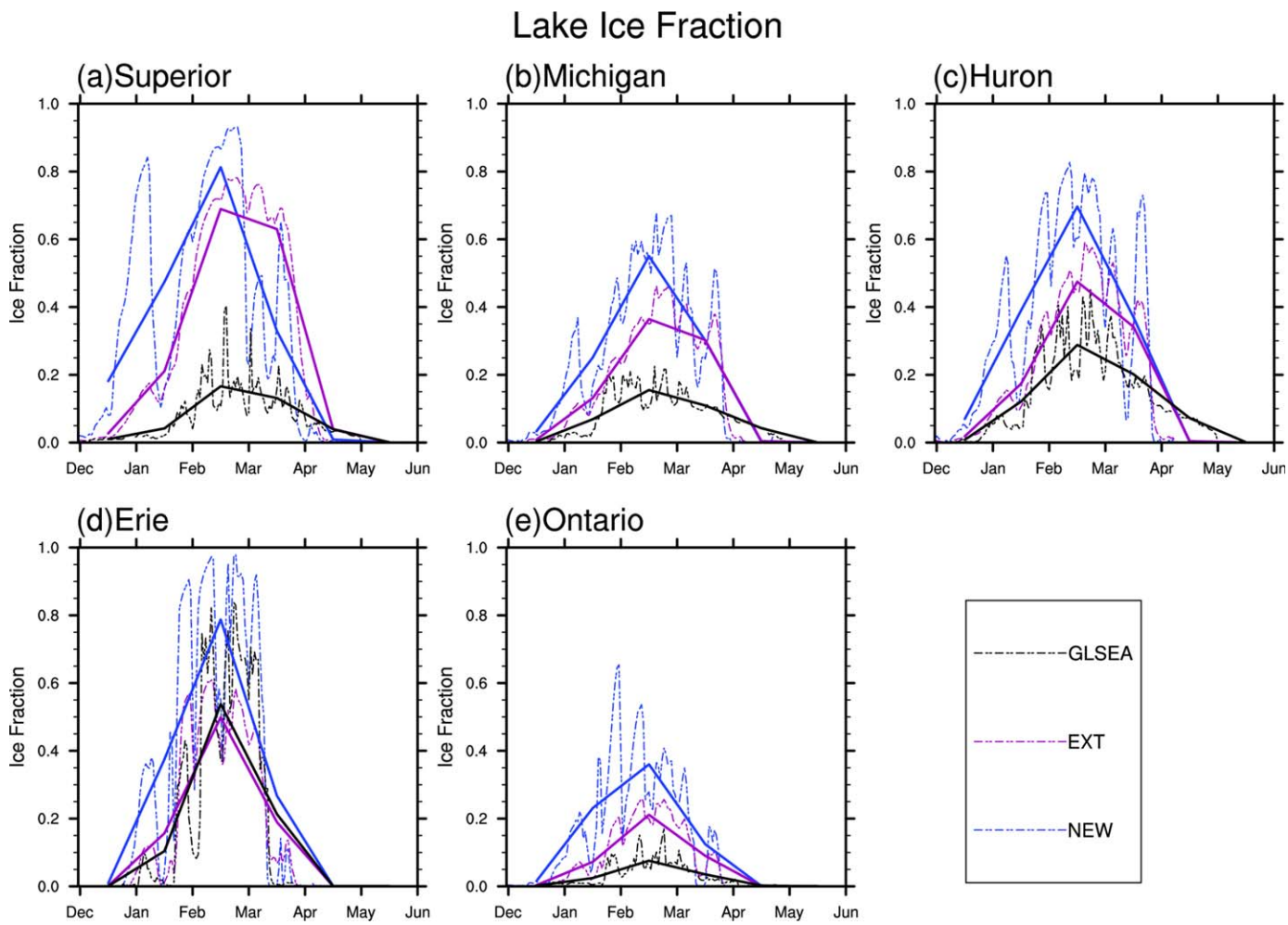

Figure 10. The lake-mean LIC in the winter 2012/1013 simulated by the new lake model with 10 layers (Lake_NEW) and the extra lake model with 25 layers (Lake_EXT), compared with the GLSEA observation (black). The solid curves are the monthly average of their corresponding dashed curves.

are different from the thermistor depths. The simulated water temperatures below the top layer are vertically interpolated to the thermistor depths. The 1-D lake model possessed a decent capability to simulate the seasonal variability of subsurface lake temperature in the location where the lake depth reaches more than 100 m, except for some biases in the magnitude. Since only the surface albedo was changed in the new lake model, the profiles of subsurface temperatures in Lake_NEW were very close to that in Lake_CLT, except for the near surface layer in the winter time when the LIC was reduced in Lake_NEW. Furthermore, we compared other vertical profiles in different lakes (Figure 9). Lake_NEW and Lake_CTL generally produced very similar subsurface temperatures.

4.5. Extralayer Experiment

All of the above experiments were performed with 10 vertical lake layers. As introduced in section 4.2, the top model layer has a thickness of 0.1 m. In one particular case when the ice fraction becomes 100%, it means the entire layer is iced. However, the reality is that in shallow areas, especially in Lake Erie, the ice thickness can reach far more than 0.1 m [*Fujisaki et al.*, 2013]. At such points, a 10-layer lake model is insufficient to present the ice physics in the Great Lakes. Thus, another experiment with more vertical layers has been conducted (Table 3). In the Lake_EXT experiment, 25 vertical layers were utilized with top three layers centered at 0.05, 0.15, and 0.25 m, respectively. The thicknesses of the three layers are 0.1 m. The ice fraction is averaged in the top three layers. Figure 10 depicts the comparison of the lake-mean LIC simulated by Lake_NEW and Lake_EXT. The LIC was reduced in Lake_EXT in all lakes, not only the monthly-mean

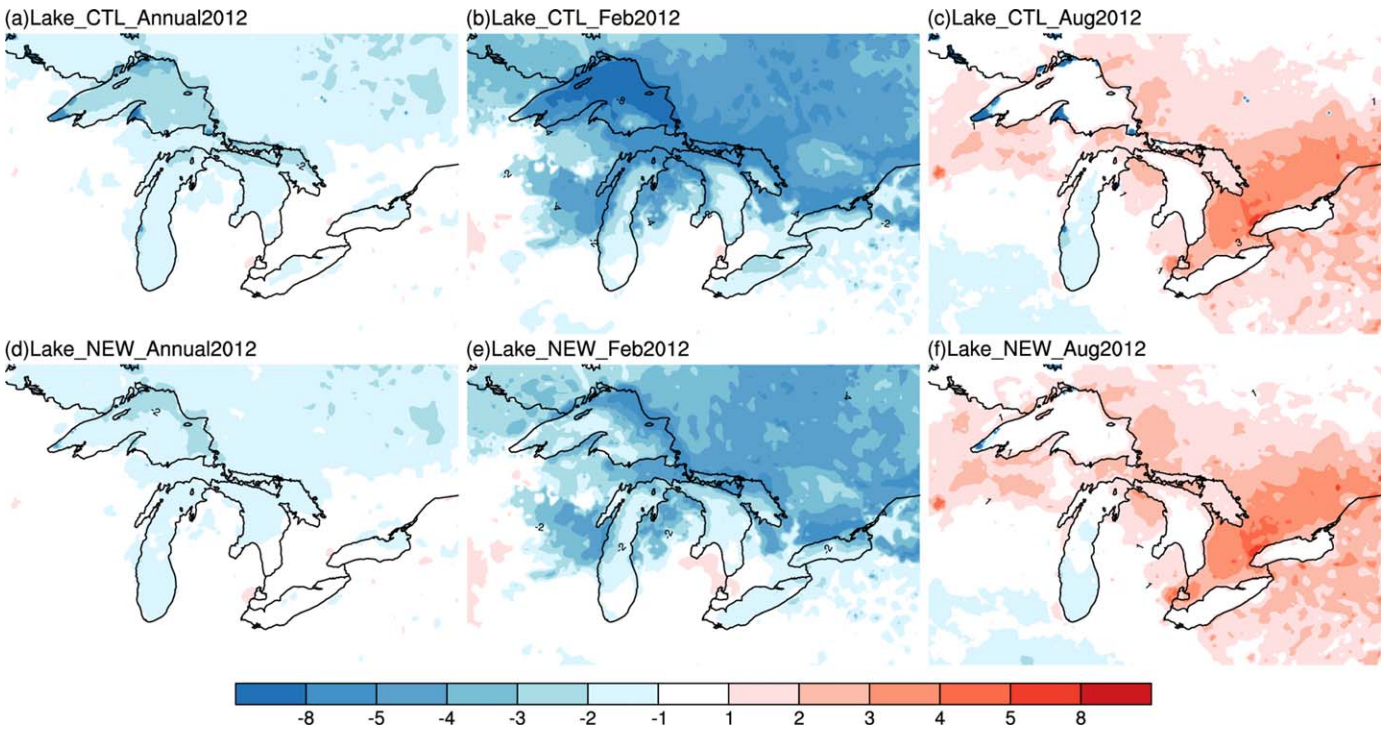

Figure 11. Air temperature (T2m, °C) differences between the WRF-lake model simulations and NARR reanalysis (model-reanalysis). The 2012 annual T2m are in the left column, the 2012 February mean T2m in the middle column, and the 2012 August mean T2m in the right column.

magnitude but also the interseasonal fluctuation. Still, more ice was produced by the 1-D lake model in deep lakes relative to the GLSEA observation.

4.6. Effects on Regional Climate

The previous comparison of coupled WRF-lake experiments demonstrates that the new lake model improves the simulations of lake surface temperature and lake ice coverage. In this section, the effect of the lake component on the atmospheric component in the coupled modeling system is further analyzed from the perspective of air temperature and precipitation.

Before showing the difference of air temperature at 2 m (T2m) among four modeling experiments, the simulated T2m was evaluated against the NARR reanalysis (Figure S1 in Supporting Information). Generally, all WRF-lake experiments are capable of reproducing the monthly or annual mean T2m except for some cold (warm) bias in winter (summer). With the calibration of *Gu et al.* [2015], the default lake model in WRF (Lake_CTL) reduced the over-lake T2m bias, especially in southern Lake Michigan, relative to Lake_OLD and Lake_CLM. To simplify the comparison, we only compared the difference between Lake_CTL and Lake_NEW experiments. Figure 11 shows the T2m discrepancy between the WRF-lake model simulations and NARR reanalysis. In February, the WRF model had a cold bias in almost the entire Great Lake region, more obviously in the northeast side. The model bias in the high latitude during the cold season could come from oversimplified snow physics in the land surface model [e.g., *Chen et al.*, 2014]. In August, a warm bias in the north and a week cold bias in the southwest were produced by WRF. In the annual mean, because of the cancelation between cold bias in winter and warm bias in summer, the overall model bias became much smaller. Specifically, the over-lake model bias in winter was significantly reduced in the Lake_NEW experiment (Figure 11e), compared to Lake_CTL (Figure 11b), especially over the deep lakes. Meanwhile, the T2m in the southern Ontario was also improved, indicating the Great Lakes' remote effect on the overlying atmosphere.

In addition to air temperature, precipitation from the WRF-lake experiments was also assessed against observations. Considering substantial uncertainties in both observations and simulations of precipitation, especially in the form of snowfall, accurately modeling precipitation still remains a considerable challenge. Multiple precipitation data sets were used to evaluate the model's performance (Figure S2 in Supporting

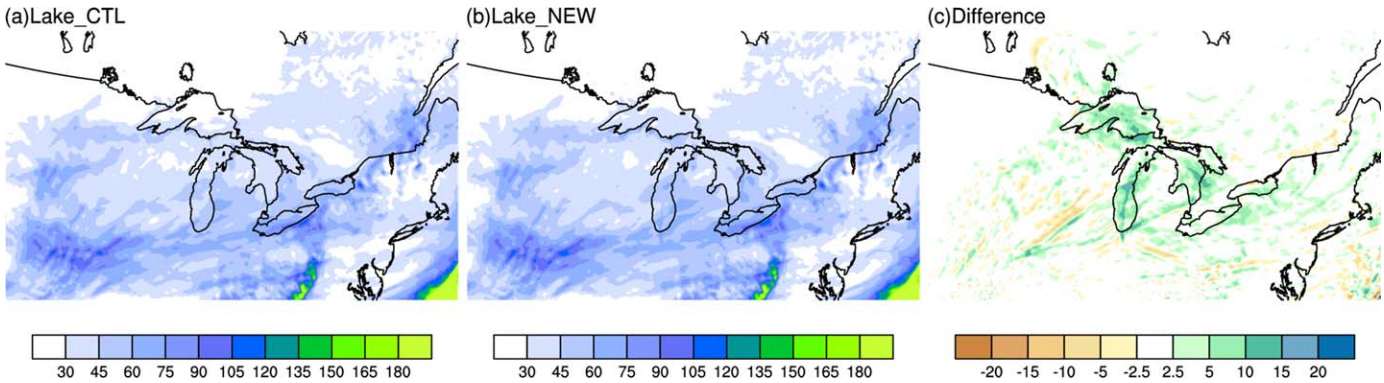

Figure 12. Domain-wide mean precipitation (mm) in February 2012 simulated by WRF-lake experiments and their difference (Lake_NEW-Lake_CTL).

Information). CMAP and GPCP on a 2.5° global grid are much coarser than the WRF model, while the 1 km DayMet covering only the land portion is upscaled to the 10 km WRF grid. In the annual mean precipitation, the Great Lakes region is characterized with a strong southeast-northwest precipitation gradient. An enhanced precipitation band along Appalachian Mountains in DayMet (Figure S2g), which is barely seen in the two coarse observations, is produced in the WRF experiments, though the WRF model tends to overestimate the precipitation magnitude. To reveal the effect of LST differences on the regional climate, especially the lake-effect snow, the precipitation in February 2012 in Lake_NEW is compared with that in Lake_CTL experiment (Figure 12). In the current resolution, the phenomenon of lake-effect precipitation along the downwind shore lines is well captured by the WRF model, which becomes more predominant along Lake Erie. With the updated lake albedo scheme, more precipitation is produced in the Great Lakes region, causing enhanced lake-effect snow in the cold season, because of reduced ice coverage in the Lake_NEW experiment.

5. Conclusions

Much effort has been devoted to improving the lake model [*Hostetler and Bartlein*, 1990; *Subin et al*., 2012; *Gu et al*., 2015], but it still remains a considerable challenge to adequately simulate lake temperature and ice in deep lakes [e.g., *Mallard et al*., 2015]. In this study, the 1-D lake model within the WRF v3.6.1 has been investigated in the Great Lakes.

In the default 10-layer lake model, the albedos of water and ice are specified with constant values, 0.08 and 0.6, respectively, ignoring effects from solar zenith angle, shortwave radiation diffusion, ice melting, and snow. Some modifications have been added to the lake model, including a dynamic lake surface albedo with a special treatment of snow cover over lake ice. Four numerical experiments have been carried out to evaluate the performances of different lake schemes in the Great Lakes (Table 3): Lake_CTL with the default scheme; Lake_OLD with the original eddy diffusivity; Lake_CLM with enhanced eddy diffusivity; Lake_NEW with the updated albedo scheme; and Lake_EXT with 25 vertical layers. The 1-D lake model is capable of capturing the seasonal variability of lake temperature and lake ice. However, it produces an early warming and quick cooling of LST in deep lakes, and excessive and early persistent LIC in all lakes. Increasing vertical diffusivity can reduce the bias in the 1-D lake model, but only in a limited way. After incorporating a dynamic lake surface albedo, the new lake model produces a more reasonable LST than the default. More impressively, the LIC is significantly reduced in the new lake model, indicating that the processes of ice melting and snow accumulation are important to simulate lake ice in the Great Lakes.

Even though substantial improvements have been demonstrated in the new model, only improving the surface processes cannot thoroughly eliminate the overall shortcomings of the 1-D lake model because of the missing horizontal mixing and ice movement. We investigated other relative researches for the Great Lakes, such as stand-alone *LISSS* [*Subin et al*., 2012], WRF/FLake [*Gula and Peltier*, 2012], and RegCM4/1-D Lake [*Bennington et al*., 2014]. Certain model biases widely exist in current lake models, although substantial improvement has been achieved. Increasing eddy diffusivity can delay the spring warm-up and fall cool-down, bringing the model closer to observations. The current effort is to improve the 1-D model in a coupled

WRF-lake modeling system, while the real nature in the lake is three-dimensional and contemporaneous with overlying atmosphere and underlying sediments. As to the ice simulation, currently the ice/snow scheme and associated phrase change process are much simplified in the 1-D lake model. The ill-solved lake ice/snow in the 1-D lake model could worsen the simulation of stratification process in early spring time because of the ice/snow-albedo feedback. The presence or absence of snow insulation can cause greater than 30 W m^{-2} monthly average changes in lake energy exchanges in the winter and summer [*Subin et al.*, 2012]. Future work is needed to improve the treatment of lake ice during periods of marginal ice cover.

Meanwhile, 3-D lake dynamical models are being developed in the Great Lakes, but they are currently staying in the off-line stage. Coupled models can not only serve as a key tool for supplementing observations in areas where the ordinary gauge network is coarse or nonexistent, but can also provide the dynamics of the air-lake-ice interaction, which becomes especially crucial to understanding climate and climate change in water-dominated areas. In order to reproduce the fidelity of lake temperature, ice, and stratification, future efforts should be dedicated to applying a fully coupled air-lake-ice model in which a 3-D lake model is utilized to represent the Great Lakes' circulation.

Acknowledgments
The authors acknowledge the NOAA Research and Development High Performance Computing Program for providing computing and storage resources that have contributed to the research results reported within this paper (http://rdhpcs.noaa.gov). We thank Dr. Dmitry Beletsky for valuable comments, and Dr. Nathan Hawley for providing the mooring data in Lake Michigan. Special thanks to Nicole Rice for editing this paper. Figures are created with the NCAR Command Language (Version 6.3.0) [Software]. [2016]. Boulder, Colorado: UCAR/NCAR/CISL/VETS. http://dx.doi.org/10.5065/D6WD3XH5. All data and codes in this paper are available upon request to Dr. Chuliang Xiao (cxiao@umich.edu). The comments of two anonymous reviewers led to improvements in the quality of this manuscript. This research is funded by the US Environmental Protection Agency's Great Lakes Restoration Initiative (GLRI), awarded to Cooperative Institute for Limnology and Ecosystems Research (CILER) through the NOAA Cooperative Agreement with the University of Michigan (NA12OAR4320071). This is the NOAA Great Lakes Environmental Research Laboratory Contribution Number 1844 and CILER contribution 1102.

References

Adler, R. F., et al. (2003), The version-2 Global Precipitation Climatology Project (GPCP) monthly precipitation analysis (1979–present), *J. Hydrometeorol*, *4*, 1147–1167.

Andreadis, K. M., P. Storck, and D. P. Lettenmaier (2009), Modeling snow accumulation and ablation processes in forested environments, *Water Resour. Res.*, *45*, W05429, doi:10.1029/2008WR007042.

Bai, X. Z., J. Wang, D. J. Schwab, Y. Yang, L. Luo, G. A. Leshkevich, and S. Z. Liu (2013), Modeling 1993–2008 climatology of seasonal general circulation and thermal structure in the Great Lakes using FVCOM, *Ocean Modell.*, *65*, 40–63, doi:10.1016/J.Ocemod.2013.02.003.

Bates, G. T., F. Giorgi, and S. W. Hostetler (1993), Toward the simulation of the effects of the Great Lakes on regional climate, *Mon. Weather Rev.*, *121*, 1373–1387.

Beletsky, D., D. Schwab, and M. McCormick (2006), Modeling the 1998–2003 summer circulation and thermal structure in Lake Michigan, *J. Geophys. Res.*, *111*, C10010, doi:10.1029/2005JC003222.

Beletsky, D., N. Hawley, and Y. R. Rao (2013), Modeling summer circulation and thermal structure of Lake Erie, *J. Geophys. Res. Oceans*, *118*, 6238–6252, doi:10.1002/2013JC008854.

Bennington, V., M. Notaro, and K. D. Holman (2014), Improving climate sensitivity of deep lakes within a regional climate model and its impact on simulated climate, *J. Clim.*, *27*, 2886–2911.

Changnon, S. A., and D. M. A. Jones (1972), Review of the influences of the Great Lakes on weather, *Water Resour. Res.*, *8*, 360–371.

Chen, F., et al. (2011), The integrated WRF/urban modelling system: Development, evaluation, and applications to urban environmental problems, *Int. J. Climatol.*, *31*, 273–288, doi:10.1002/joc.2158.

Chen, F., C. Liu, J. Dudhia, and M. Chen (2014), A sensitivity study of high-resolution regional climate simulations to three land surface models over the western United States, *J. Geophys. Res. Atmos.*, *119*, 7271–7291, doi:10.1002/2014JD021827.

Collins, W. D., P. J. Rasch, B. A. Boville, J. J. Hack, J. R. McCaa, D. L. Williamson, J. T. Kiehl, and B. Briegleb (2004), Description of the NCAR Community Atmosphere Model (CAM 3.0), *Tech. Rep. NCAR TN-464+STR*, Natl. Cent. for Atmos. Res., Boulder, Colo.

Cox, H. J. (1917), Influence of the Great Lakes upon movement of high and low pressure areas, in *Proceedings of the Second Pan American Scientific Congress*, vol. *2*, edited by G. L. Swiggert, pp. 432–459, Gov. Print. Off., Washington, D. C.

Croley, T. E., II (1989), Verifiable evaporation modeling on the Laurentian Great Lakes, *Water Resour. Res.*, *25*(5), 781–792.

Dupont, F., P. Chittibabu, V. Fortin, Y. R. Rao, and Y. Lu (2012), Assessment of a NEMO-based hydrodynamic modeling system for the Great Lakes, *Water Qual. Res. J. Can.*, *47*, 198–214, doi:10.2166/wqrjc.2012.014.

Fang, X., and H. G. Stefan (1996), Long-term lake water temperature and ice cover simulations/measurements, *Cold Reg. Sci. Technol.*, *24*, 289–304, doi:10.1016/0165?232X(95)00022?4.

Fujisaki, A., J. Wang, X. Bai, G. Leshkevich, and B. Lofgren (2013), Model-simulated interannual variability of Lake Erie ice cover, circulation, and thermal structure in response to atmospheric forcing, 2003–2012, *J. Geophys. Res. Oceans*, *118*, 4286–4304, doi:10.1002/jgrc.20312.

Goyette, S., N. A. McFarlane, and G. M. Flato (2000), Application of the Canadian Regional Climate Model to the Laurentian Great Lakes region: Implementation of a lake model, *Atmos. Ocean*, *38*, 481–503.

Gu, H., J. Jin, Y. Wu, M. B. Ek, and Z. M. Subin (2015), Calibration and validation of lake surface temperature simulations with the coupled WRF-lake model, *Clim. Change*, *129*, 471–485, doi:10.1007/s10584-013-0978-y.

Gula, J., and W. R. Peltier (2012), Dynamical downscaling over the Great Lakes basin of North America using the WRF regional climate model: The impact of the Great Lakes system on regional greenhouse warming, *J. Clim.*, *25*, 7723–7742.

Henderson-Sellers, B. (1985), New formulation of eddy diffusion thermocline models, *Appl. Math. Modell.*, *9*, 441–446.

Hong, S.-Y., and J.-O. J. Lim (2006), The WRF single-moment 6-class microphysics scheme (WSM6), *J. Korean Meteorol. Soc.*, *42*, 129–151.

Hong, S.-Y., Y. Noh, and J. Dudhia (2006), A new vertical diffusion package with an explicit treatment of entrainment processes, *Mon. Weather Rev.*, *134*(9), 2318–2341, doi:10.1175/MWR3199.1.

Hostetler, S. W., and P. J. Bartlein (1990), Simulation of lake evaporation with application to modeling lake level variations of Harney-Malheur Lake, Oregon, *Water Resour. Res.*, *26*(10), 2603–2612.

Hostetler, S. W., G. T. Bates, and F. Giorgi (1993), Interactive coupling of a lake thermal model with a regional climate model, *J. Geophys. Res.*, *98*(D3), 5045–5057, doi:10.1029/92JD02843.

Huang, A., Y. R. Rao, and Y. Lu (2010), Evaluation of a 3-D hydrodynamic model and atmospheric forecast forcing using observations in Lake Ontario, *J. Geophys. Res.*, *115*, C02004, doi:10.1029/2009JC005601.

Kain, J. S. (2004), The Kain–Fritsch convective parameterization: An update, *J. Appl. Meteorol.*, *43*, 170–181.

Kourzeneva, E., H. Asensio, E. Martin, and S. Faroux (2012), Global gridded dataset of lake coverage and lake depth for use in numerical weather prediction and climate modelling, *Tellus, Ser. A*, *64*, 1–14.

Lofgren, B. M. (1997), Simulated effects of idealized Laurentian Great Lakes on regional and large-scale climate, *J. Clim.*, *10*, 2847–2858.
Lofgren, B. M. (2004), A model for simulation of the climate and hydrology of the Great Lakes Basin, *J. Geophys. Res.*, *109*, D18108, doi: 10.1029/2004JD004602.
MacKay, M. D., et al. (2009), Modeling lakes and reservoirs in the climate system, *Limnol. Oceanogr.*, *54*, 2315–2329.
Mallard, M. S., C. G. Nolte, O. R. Bullock, T. L. Spero, and J. Gula (2014), Using a coupled lake model with WRF for dynamical downscaling, *J. Geophys. Res. Atmos.*, *119*, 7193–7208, doi:10.1002/2014JD021785.
Mallard, M. S., C. G. Nolte, T. L. Spero, O. R. Bullock, K. Alapaty, J. A. Herwehe, J. Gula, and J. H. Bowden (2015), Technical challenges and solutions in representing lakes when using WRF in downscaling applications, *Geosci. Model Dev.*, *8*, 1085–1096, doi:10.5194/gmd-8-1085-2015.
Martynov, A., L. Sushama, and R. Laprise (2010), Simulation of temperate freezing lakes by one-dimensional lake models: Performance assessment for interactive coupling with regional climate models, *Boreal Environ. Res.*, *15*, 143–164.
McCormick, M. J., and J. D. Pazdalski (1993), Monitoring midlake water temperature in southern Lake Michigan for climate change studies, *Clim. Change*, *25*, 119–125, doi:10.1007/BF01661201.
Mesinger, F., et al. (2006), North American regional reanalysis, *Bull. Am. Meteorol. Soc.*, *87*, 343–360, doi:10.1175/BAMS-87-3-343.
Mironov, D., L. Rontu, E. Kourzeneva, and A. Terzhevik (2010), Towards improved representation of lakes in numerical weather prediction and climate models: Introduction to the special issue of Boreal Environment Research, *Boreal Environ. Res.*, *15*, 97–99.
Notaro, M., K. Holman, A. Zarrin, E. Fluck, S. Vavrus, and V. Bennington (2013), Influence of the Laurentian Great Lakes on regional climate, *J. Clim.*, *26*, 789–804.
Oleson, K. W., et al. (2013), Technical description of version 4.5 of the Community Land Model (CLM), *NCAR Tech. Note NCAR/TN-503+STR*, 422 pp., Natl. Cent. for Atmos. Res., Boulder, Colo., doi:10.5065/D6RR1W7M.
Pivovarov, A. A. (1972), *Thermal Conditions in Freezing Lakes and Reservoirs*, John Wiley, New York.
San Jose, R., J. L. Perez, and R. M. Gonzalez (2011), Sensitivity analysis of two different shadow models implemented into EULAG CFD model Madrid experiment, *Res. J. Chem. Environ.*, *15*, 1–8.
Schwab, D., G. Leshkevich, and G. Muhr (1992), Satellite measurements of surface water temperature in the Great Lakes: Great Lakes Coastwatch, *J. Great Lakes Res.*, *18*, 247–258, doi:10.1016/S0380-1330(92)71292-1.
Scott, R. W., and F. A. Huff (1996), Impacts of the Great Lakes on regional climate conditions, *J. Great Lakes Res.*, *22*, 845–863.
Skamarock, W., J. B. Klemp, J. Dudhia, D. O. Gill, D. Barker, M. G. Duda, X.-Y. Huang, and W. Wang (2008), A description of the advanced research WRF version 3, *NCAR Tech. Note NCAR/TN-475+STR*, Mesoscale and Microscale Meteorology Division of the Natl. Cent. for Atmos. Res., Boulder, Colo., doi:10.5065/D68S4MVH.
Spero, T. L., C. G. Nolte, J. H. Bowden, M. S. Mallard, and J. A. Herwehe (2016), The impact of incongruous lake temperatures on regional climate extremes downscaled from the CMIP5 archive using the WRF model, *J. Clim.*, *29*, 839–853.
Stepanenko, V. M., S. Goyette, A. Martynov, M. Perroud, X. Fang, and D. Mironov (2010), First steps of a Lake Model Intercomparison Project: LakeMIP, *Boreal Environ. Res.*, *15*, 191–202.
Subin, Z. M., W. J. Riley, and D. V. Mironov (2012), An improved lake model for climate simulations: Model structure, evaluation, and sensitivity analyses in CESM1, *J. Adv. Model. Earth Syst.*, *4*, M02001, doi:10.1029/2011MS000072.
Thornton, P. E., M. M. Thornton, B. W. Mayer, Y. Wei, R. Devarakonda, R. S. Vose, and R. B. Cook (2016), Daymet: Daily surface weather data on a 1-km grid for North America, Version 3, report, ORNL DAAC, Oak Ridge, Tenn., doi:10.3334/ORNLDAAC/1328.
Wang, J., X. Bai, H. Hu, A. Clites, M. Colton, and B. Lofgren (2012), Temporal and spatial variability of Great Lakes ice cover, 1973–2010, *J. Clim.*, *25*, 1318–1329, doi:10.1175/2011JCLI4066.1.
Wright, D. M., D. J. Posselt, and A. L. Steiner (2013), Sensitivity of lake-effect snowfall to lake ice cover and temperature in the Great Lakes region, *Mon. Weather Rev.*, *141*, 670–689.
Xie, P., and P. A. Arkin (1997), Global precipitation: A 17-year monthly analysis based on gauge observations, satellite estimates, and numerical model outputs, *Bull. Am. Meteorol. Soc.*, *78*, 2539–2558.
Xue, P., D. J. Schwab, and S. Hu (2015), An investigation of the thermal response to meteorological forcing in a hydrodynamic model of Lake Superior, *J. Geophys. Res. Oceans*, *120*, 5233–5253, doi:10.1002/2015JC010740.